

from the reaction flask and distilled to obtain 3.5 g (0.035 mol, yield 42%) of **3** (bp 87–92 °C). This sample contained about 10% of 1,3-disilacyclopentane. Also distilled off at slightly lower temperatures were ring cleavage side products.

**Characterization and Spectroscopic Measurements.** All compounds were characterized by using nuclear magnetic resonance spectra (Varian XL-2000 and EM-390), mass spectra (VG Analytical 70S), and infrared and Raman spectra. Mid-infrared gas-phase spectra of **3** at vapor pressures of 5 and 45 Torr contained in a 10-cm gas cell with KBr windows were recorded on a Digilab FTS-60 interferometer. Liquid-phase Raman spectra were recorded with a Cary 82 monochromator equipped with a Coherent Radiation Innova 20 argon ion laser source. Detailed

spectra are available elsewhere.<sup>14</sup> Mid-infrared spectra of the combination bands in the SiH<sub>2</sub> stretching region were recorded on a Bomem DA3.002 interferometer using the 10-cm cell. The Bomem instrument was also used to acquire the far-infrared spectrum of **3**. An adjustable path length (up to 21 m) Wilks multireflectance cell was used to contain the sample for these scans. A liquid helium cooled germanium bolometer was utilized as the detector, and 1000 scans were typically coadded. In the 40–125-cm<sup>-1</sup> range, a 25 μm thick beamsplitter and a mercury lamp source were utilized.

*Acknowledgment.* We thank the National Science Foundation and the Robert A. Welch Foundation for financial support.

## Measurements of Line Strengths in the HO<sub>2</sub> ν<sub>1</sub> Overtone Band at 1.5 μm Using an InGaAsP Laser

T. J. Johnson, F. G. Wienhold, J. P. Burrows, G. W. Harris,\*

*Atmospheric Chemistry Department, Max Planck Institute for Chemistry, P.O. Box 3060, W-6500 Mainz, Germany*

and H. Burkhard

*DBP Telekom Research Institute, P.O. Box 10 00 03, W-6100 Darmstadt, Germany (Received: April 25, 1991; In Final Form: June 14, 1991)*

We report the first observation of resolved rotational–vibrational overtone (2ν<sub>1</sub>) absorptions of the hydroperoxyl radical (HO<sub>2</sub>) in the 1.5-μm region, using two-tone frequency modulation spectroscopy (TTFMS) with an InGaAsP laser diode and White-cell optics. Photolysis of Cl<sub>2</sub>/H<sub>2</sub>/O<sub>2</sub> mixtures was used to produce the HO<sub>2</sub>, and the concentration was determined by modulated-photolysis UV absorption spectroscopy. The line center absorption cross sections for the strongest lines ranged between 1.3 × 10<sup>-20</sup> and 10 × 10<sup>-20</sup> cm<sup>2</sup> molecule<sup>-1</sup> under Doppler-limited conditions. For the strongest line this corresponds to an integrated line strength *S* of 1.6 × 10<sup>-21</sup> cm<sup>2</sup> molecule<sup>-1</sup> cm<sup>-1</sup>, a line strength of the same order of magnitude as lines previously observed in the relatively weak ν<sub>1</sub> fundamental.

### Introduction

The hydroperoxyl radical, HO<sub>2</sub>, is a pivotal atmospheric species, being closely coupled to OH, the most important oxidant in both tropospheric and stratospheric chemistry.<sup>1</sup> Currently several techniques are under development to quantitatively measure atmospheric concentrations of HO<sub>2</sub> and the associated RO<sub>2</sub> family of radicals, either spectroscopically or by chemical conversion methods.<sup>2</sup> Recent improvements<sup>3</sup> in the chemical conversion method have made it much more useful, but the technique suffers from the drawback that it cannot distinguish between HO<sub>2</sub> and RO<sub>2</sub>. The detection limits appear to be ~2 pptv, slightly better than those obtained with the matrix isolation EPR techniques, one of the few spectroscopic techniques to have successfully measured tropospheric HO<sub>2</sub>.<sup>4</sup> The EPR technique is sensitive, but requires relatively long collection times (ca. 1 h) and off-line analysis in the laboratory.

Optical measurements to monitor atmospheric HO<sub>2</sub> using its UV bands are prevented by interference from adjacent O<sub>3</sub> bands and by the relative weakness of the unstructured HO<sub>2</sub> absorption. Atmospheric measurements using the mid-IR absorptions via tunable diode laser absorption spectroscopy (TDLAS) have not as yet been realized due to the small concentrations and line strengths,<sup>5,6</sup> as well as sampling problems. However, HO<sub>2</sub> is known to have a few absorption bands in the near-IR region, a vibronic progression in the low-lying <sup>2</sup>A' ← <sup>2</sup>A'' transition beginning at 1.425 μm, as well as the first vibrational overtone in the OH stretch centered at 1.504 μm. Since Hunziker and Wendt<sup>7</sup> first identified

and assigned these bands under low resolution in 1974, there has been much interest<sup>2</sup> as to the magnitude of the individual line strengths: Measuring HO<sub>2</sub> in the near-IR region is potentially more attractive than measuring in the mid-IR region because the generally weaker line strengths can in part be compensated for by measuring at higher pressures before pressure broadening becomes important. Using broader lines is also more practicable in the near-IR region because there are fewer interfering absorptions as compared to the mid-IR region. Most importantly, because two-tone frequency modulation spectroscopy (TTFMS) in the near-IR region offers the possibility of measuring at higher pressures without significant loss of signal, the use of open-path multiple reflection cells may be feasible. This would avoid the severe problems of sampling HO<sub>2</sub> at reduced pressures, which is necessary for optimum performance of a mid-IR TDL spectrometer aimed at tropospheric measurements. The 1.5-μm lasers are

(1) (a) Warneck, P. *Chemistry of the Natural Atmosphere*, Academic Press: San Diego, CA, 1988. (b) Finlayson-Pitts, B. J.; Pitts, J. N. *Atmospheric Chemistry*, Wiley-Interscience: New York, 1986.

(2) Cantrell, C. A.; Shetter, R. E.; McDaniel, A. H.; Calvert, J. G. *Measurement Methods for Peroxy Radicals in the Atmosphere*. In *Measurement Challenges in Atmospheric Chemistry*; Adv. Chem. Ser. No. 232; American Chemical Society: Washington, DC, in press. This article provides an excellent review of techniques aimed at measuring HO<sub>2</sub> and RO<sub>2</sub>.

(3) Hastie, D. R.; Weissenmayer, M.; Burrows, J. P.; Harris, G. W. *Anal. Chem.*, accepted for publication.

(4) Mihelcic, D.; Volz-Thomas, A.; Pätz, H. W.; Kley, D.; Mihelcic, M. *J. Atm. Chem.* 1990, 11, 271.

(5) Zahniser, M. S.; McCurdy, K. E.; Stanton, A. C. *J. Phys. Chem.* 1989, 93, 1066.

(6) Zahniser, M. S.; Stanton, A. C. *J. Chem. Phys.* 1984, 80, 4951.

(7) Hunziker, H. E.; Wendt, H. R. *J. Chem. Phys.* 1974, 60, 4622.

\* To whom correspondence should be addressed.

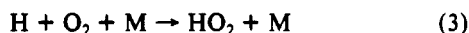
especially well suited to such an experiment due to their long mode tuning.

Although the near-IR spectra of the 1.43- and 1.51- $\mu\text{m}$  emission bands have been recorded<sup>8,9</sup> and the individual HO<sub>2</sub> lines subsequently assigned,<sup>10</sup> measurement of individual absorption lines in either the near-IR vibronic or overtone bands has eluded spectroscopists until the present. It has been demonstrated that frequency modulation spectroscopy in combination with either 1.3- or 1.5- $\mu\text{m}$  diode lasers is capable of detecting optical densities  $\sim 10^{-6}$  on a routine basis.<sup>11-14</sup> We have recently constructed such a two-tone frequency modulation (TTFM) spectrometer and report here preliminary measurements of the absorption cross sections of several lines observed within the  ${}^2A''(200) \leftarrow {}^2A''(000)$  overtone band of HO<sub>2</sub> near 1.5  $\mu\text{m}$ .

### Experimental Section

The TTFM spectrometer used in these experiments has been described in some detail.<sup>14</sup> Improvements to the spectrometer that have lowered the detection limits will be described elsewhere. Briefly, a 1.5- $\mu\text{m}$  InGaAsP diode laser was modulated by two radio frequencies  $\nu_m \pm \frac{1}{2}\Omega$ , with  $\nu_m$  typically 500 MHz and  $\frac{1}{2}\Omega$  typically 1-5 MHz, producing sidebands on the laser carrier frequency. The modulated laser beam was sent through a 1.5-m base length White cell (working path length 132 m) and focused onto a high speed detector, the signal being retrieved at the beat frequency  $\Omega$  as the laser is scanned through an absorption line. Due to impedance matching and filter considerations, the frequencies used in these experiments were  $\nu_m = 525.4$  MHz and  $\frac{1}{2}\Omega = 5.5$  MHz with the beat signal detected at  $\Omega = 11.0$  MHz. The distributed feedback (DFB) laser used for the measurements was an InGaAsP/InP diode of the constricted-mesa type.<sup>15</sup> These lasers allow much more optical power to be coupled into a single mode (i.e., greater monochromaticity), but can only be tuned over a rather limited wavelength range. The particular diode used had an intrinsic line width of  $\Delta\nu = 15$  MHz and a sidemode suppression ratio  $>37$  dB. As is typical for these lasers, the total power was high, over 3 mW, of which slightly less than 1 mW was collected by the  $f/2.2$  collimating off-axis paraboloid (OAP); the power monitored at the detector after the beam passed through the White cell was typically of the order of 55  $\mu\text{W}$ . The number of passes through the White cell was selected such that the power at the detector remained sufficiently high for the shot noise to dominate the detector and electronics noise. Absorption wavelengths were measured separately by using a low-resolution (1.0  $\text{cm}^{-1}$ ) monochromator.

HO<sub>2</sub> production was initiated by irradiation of Cl<sub>2</sub>/H<sub>2</sub>/air mixtures, using (up to) six TLD-36W/08 lamps mounted in a polished metal housing surrounding a glass White cell as described elsewhere.<sup>16</sup> HO<sub>2</sub> was produced by the reaction of the photo-generated chlorine atoms with the H<sub>2</sub>/O<sub>2</sub> mixture:



Hydroperoxyl radical concentrations were measured by monitoring the modulated absorption at  $\lambda = 220$  nm with a signal averager: The UV cross section used was the recently confirmed  $\sigma_{220} = 340 \times 10^{-20} \text{ cm}^2 \text{ molecule}^{-1}$  value of Crowley et al.<sup>17</sup> Pressures used

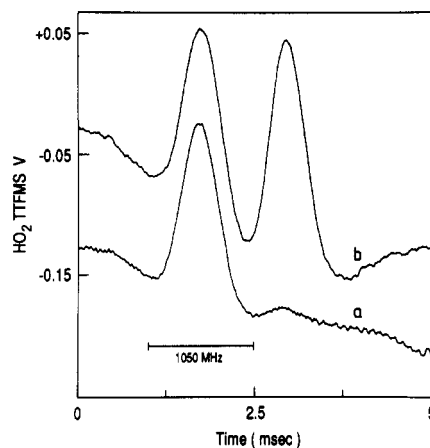


**Figure 1.** TTFM spectra recorded near 1.5083  $\mu\text{m}$ , with six photolysis black lamps on (upper trace) and off (lower trace). The line to the left is due to residual H<sub>2</sub>O, the line to the right due to HO<sub>2</sub>. The ordinate and abscissa for the two spectra are the same, the "lights off" spectrum vertically shifted for clarity. The HO<sub>2</sub> optical density corresponds to  $4.0 \times 10^{-4}$ , and the horizontal bar corresponds to  $2\nu_m = 1050$  MHz.

for the experiments ranged between 50 and 120 Torr, HO<sub>2</sub> signals maximizing at values near  $\sim 60$  Torr.

Certain precautions were taken to ensure that the near-IR absorption lines observed indeed belong to HO<sub>2</sub>: When the Cl<sub>2</sub> was removed from the system with all other parameters held constant, the modulated near-IR signals naturally disappeared. Also, the real-time oscilloscope TTFMS signal closely followed the duty cycle of the photolysis black lamps. To study the time dependence of the signals more quantitatively, the near-infrared detector mixer output at line center was connected to the signal averager, which was triggered by the molecular modulation photolysis lamps, and the signal monitored the same way as for the UV signal. The near-IR signal time dependence agreed with the UV-signal behavior. To rule out that the near-IR absorptions were due to, for example, H<sub>2</sub>O<sub>2</sub>, a static mixture was also subjected to the same photolysis cycle. The near-IR absorptions did not steadily increase but rather continued to follow the modulation cycle, and must therefore be due to a short-lived intermediate species, thus ruling out H<sub>2</sub>O<sub>2</sub> and HCl. In this wavelength region ( $6630 \text{ cm}^{-1}$ ), virtually all absorptions are due to vibrational overtones or combination bands: since there were no C-containing species in the system, the number of possible photochemical intermediates that may absorb here is effectively limited to HO<sub>2</sub> (and OH), and these experiments thus confirm the low-resolution work of Hunziker and Wendt.<sup>7</sup>

### Results

The laser temperature was varied between approximately 286 and 303 K, and the strongest photoactive absorptions were recorded. Typical TTFM spectra recorded with the photolysis lamps off and on, respectively, are displayed in Figure 1a,b. A small sinusoidal signal due to a White-cell étalon is seen in both scans, even though an electronic low-pass filter was placed after the mixer output as suggested by Cooper.<sup>18</sup> The HO<sub>2</sub> rovibronic line strengths were calculated as follows: The optical density of a convenient H<sub>2</sub>O absorption line at known pressure was measured in direct transmission mode ( $P_{\text{H}_2\text{O}} = 0.329$  Torr,  $\text{OD} = 6.90 \times 10^{-2}$ ) and used to calibrate the TTFMS signal for H<sub>2</sub>O. Because these optical densities were large, a calibrated-step attenuator was used to keep the detected signal within the dynamic range of the RF mixer. Extrapolation to smaller optical densities is possible, since the TTFMS signal has been empirically shown<sup>18</sup> to be linear in absorption strength over several orders of magnitude. This H<sub>2</sub>O calibration factor was then used to calculate the HO<sub>2</sub> optical densities, taking into account the correction for line widths (vide

(8) Becker, K. H.; Fink, E. H.; Langen, P.; Schurath, U. *J. Chem. Phys.* **1974**, *60*, 4623.

(9) Giachardi, D. J.; Harris, G. W.; Wayne, R. P. *Chem. Phys. Lett.* **1975**, *37*, 586.

(10) (a) Freedman, P. A.; Jones, W. J. *J. Chem. Soc., Faraday Trans. 2* **1976**, *72*, 207. (b) Tuckett, R. P.; Freedman, P. A.; Jones, W. J. *Mol. Phys.* **1979**, *37*, 379.

(11) Stanton, A. C.; Silver, J. A. *Appl. Opt.* **1988**, *27*, 5009.

(12) Carlisle, C. B.; Cooper, D. E. *Opt. Lett.* **1989**, *14*, 1306.

(13) Carlisle, C. B.; Cooper, D. E. *Appl. Phys. Lett.* **1990**, *56*, 805.

(14) Johnson, T. J.; Wienhold, F. G.; Burrows, J. P.; Harris, G. W. *Appl. Opt.* **1991**, *30*, 407.

(15) Hillmer, H.; Hansmann, S.; Burkhard, H. *Appl. Phys. Lett.* **1990**, *57*, 534.

(16) Burrows, J. P.; Tyndall, G. S.; Moortgat, G. K. *J. Phys. Chem.* **1985**, *89*, 4848.

(17) Crowley, J. N.; Simon, F. G.; Burrows, J. P.; Moortgat, G. K.; Jenkin, M. E.; Cox, R. A. *J. Photochem.*, in press.

(18) Carlisle, C. B.; Cooper, D. E.; Preier, H. *Appl. Opt.* **1989**, *28*, 2567.

TABLE I: HO<sub>2</sub> Absorption Wavelengths and Cross Sections

line no.	λ, μm	10 <sup>20</sup> σ, cm <sup>2</sup> molecule <sup>-1</sup>	line no.	λ, μm	10 <sup>20</sup> σ, cm <sup>2</sup> molecule <sup>-1</sup>
1	1.5082	6.2	13	1.5089	4.5
2	1.5082	5.3	14	1.5090	10.4
3	1.5083	3.2	15	1.5090	9.4
4	1.5083	3.0	16	1.5092	5.6
5	1.5085	7.3	17	1.5093	3.8
6	1.5086	3.4	18	1.5093	1.9
7	1.5086	1.3	19	1.5093	4.5
8	1.5086	1.5	20	1.5095	3.2
9	1.5086	2.3	21	1.5095	7.0
10	1.5086	3.6	22	1.5097	2.6
11	1.5088	5.3	23	1.5097	2.3
12	1.5088	2.7			

\* Wavelengths are accurate to approximately 0.5 nm.

infra). The water line used for calibration is coincidentally adjacent to one of the HO<sub>2</sub> lines and is to be seen in Figure 1, due to trace amounts of water degassing from the cell walls.

In TTFMS, the frequency spacing between the central peak and the negative flanks of the recorded spectrum depends only on the rf modulation frequency  $\nu_m$ , and  $\nu_m$  thus provides an internal frequency calibration. The horizontal bar spanning the two negative flanks in Figure 1 thus represents twice the  $\nu_m$  frequency, 1050.8 MHz. It has been shown that there is no loss of TTFM signal so long as  $\nu_m > \Gamma_{\text{fwhm}}$  where  $\Gamma$  is the absorption feature line width.<sup>19</sup> Although this condition was satisfied for the HO<sub>2</sub> spectra ( $\nu_m = 525.4$  MHz  $> \Gamma_{\text{fwhm,HO}_2} = 428$  MHz), the TTFMS signal for water was not fully maximized: ( $\nu_m = 525.4$  MHz  $< \Gamma_{\text{fwhm,H}_2\text{O}} = 579$  MHz). The TTFM spectrometer therefore had slightly different sensitivities for H<sub>2</sub>O and HO<sub>2</sub>, and a corresponding small correction (10%) had to be applied in calculating the  $\sigma_{\text{HO}_2}$  values shown in Table I.

The HO<sub>2</sub> and H<sub>2</sub>O signals displayed in Figure 1 correspond to optical densities of  $(4-5) \times 10^{-4}$ . The 5-ms scan was averaged 500 times on an EG&G signal averager for a  $<3$ -s data collection time, the S/N ratio being  $\geq 100$ . The bandwidth of the low-pass filter used for étalon suppression was not measured exactly for these spectra, but from similar data the effective measurement bandwidth can be estimated as  $\Delta f_{\text{eff}} \sim 5$  Hz. We note that optical densities  $< 8 \times 10^{-5}$  could be observed on the spectrometer oscilloscope in real time, greatly facilitating the search for weak transient absorptions. The TTFMS signals, laser powers, and HO<sub>2</sub> concentrations for a series of lines were recorded, and the resulting absorption cross sections  $\sigma$  are presented with the approximate wavelengths in Table I. There are several sources of uncertainty in the tabulated  $\sigma$  values. In addition to uncertainties in the TTFMS calibration, there were changes in [HO<sub>2</sub>] during the course of the experiment due to instabilities in pressure and photolysis rates. Also, diode lasers vary not only their wavelength, but also their output power  $I_0$  as the diode current and temperature are changed, and  $I_0$  needed to be measured separately for each HO<sub>2</sub> line, the correction introducing a further small error. Acknowledging these experimental uncertainties, we believe the  $\sigma$  values of Table I may only be accurate to about 50%. The lines reported here are presumably all within the P branch of the overtone transition, but the wavelengths must be measured more accurately in order to assign the lines within the band. Such an assignment would enable a calculation of the band strength for the  ${}^2A''(200) \leftarrow {}^2A''(000)$  transition. Experiments to measure both  $\lambda$  and  $\sigma$  more accurately are currently in progress.

To make a test of the detection limit under Doppler broadened conditions, one of the strongest lines (line 15, Table I) was selected and the HO<sub>2</sub> concentration reduced at constant pressure by reducing the photolysis rate. An absolute HO<sub>2</sub> concentration was established by using the UV signal with six photolysis lamps. With only one lamp, however, the TTFMS signal was still too strong to make a realistic estimate of the detection limit in a 1-Hz bandwidth (1320 Hz low-pass, average of 1320 scans). Indeed,

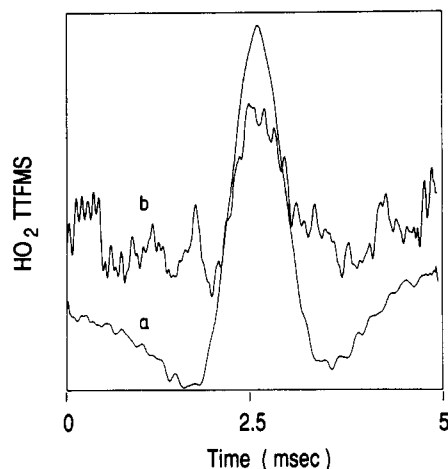


Figure 2. TTFMS signal due to an HO<sub>2</sub> line at 1.5090 μm with one photolysis lamp on (a) and due only to sunlight photolysis (b). Trace b was obtained by recording two successive spectra with the window shades open and closed, respectively, and subtracting. The resulting spectrum was smoothed once. The 5-ms total scans were each averaged 1320 times for an effective measurement bandwidth of 1 Hz.

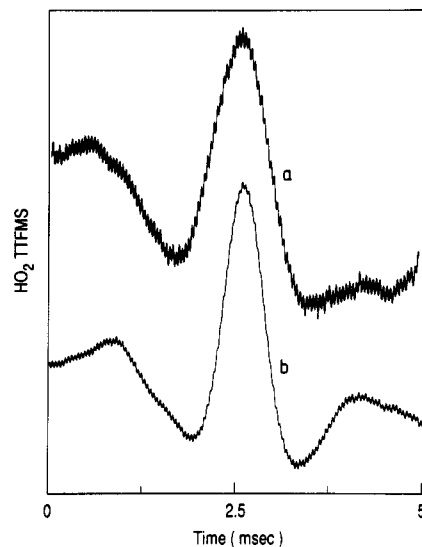


Figure 3. TTFMS signal due to an HO<sub>2</sub> line at 1.5090 μm. Curve a was recorded at 173.1 Torr, curve b at 62.7 Torr. The ordinate was adjusted to display approximately the same size signal; the HO<sub>2</sub> TTFMS signal was lower by a factor of  $\sim 2.5$  at higher pressure. The 5-ms scans were each averaged 500 times.

the one black lamp spectrum is the "reference" spectrum of Figure 2. It was found that the late afternoon sunlight in the laboratory was sufficient to photolyze enough Cl<sub>2</sub> to generate a measurable HO<sub>2</sub> signal; Figure 2b was obtained by recording two successive spectra, room shades open and closed, respectively, subtracting the two, and smoothing the result by using a 13-channel running average. The spectrum in Figure 2a, which arises from  $3.9 \times 10^{11}$  HO<sub>2</sub> cm<sup>-3</sup>, was used as a calibration for spectrum 2b. The least-squares fit yielded an HO<sub>2</sub> concentration of [HO<sub>2</sub>] =  $(1.6 \pm 0.3) \times 10^{10}$  cm<sup>-3</sup> for spectrum b, whereby the fit error is one standard deviation. The ratio of the signal to the root-mean-square amplitude of the residuals was  $\sim 10$ . We therefore estimate the detection limit of our spectrometer as  $\sim 1.5 \times 10^9$  HO<sub>2</sub> cm<sup>-3</sup> for a 60 Torr measurement pressure. This detection limit corresponds to an optical density of  $\sim 2 \times 10^{-6}$  and a mixing ratio of  $\sim 1$  ppb in a 1-Hz bandwidth with a 132-m path length.

In order to extrapolate the instrument performance to higher measurement pressures, we briefly investigated the effect of pressure broadening on the HO<sub>2</sub> lines. Figure 3 presents two spectra of an HO<sub>2</sub> absorption line recorded at 63 and 173 Torr total pressure. The HO<sub>2</sub> signal at the higher pressure was lower by a factor of 2.5 (due to the more efficient self-reaction and the

(19) Cooper, D. E.; Warren, R. E. *J. Opt. Soc. Am. B* 1987, 4, 470.

decreased efficiency of TTFMS due to pressure broadening). As discussed earlier, the frequency spacing between the negative and positive excursions in the TTFM signal is a function only of  $\nu_m$  for  $\nu_m > \Gamma_{\text{fwhm}}$ . Under such conditions,<sup>19</sup> it is the width of the central, positive-going peak that is approximately proportional to  $\Gamma_{\text{fwhm}}$  (so long as  $\Omega \ll \Gamma_{\text{fwhm}}$ , as is true here). However, for our measurements, in which  $\nu_m \approx \Gamma_{\text{fwhm}}$ , it is difficult to deconvolute the Voigt line width encoded in the TTFM signal. Figure 3 does show, however, that the width of the central feature increases by  $\sim 50\%$  between 63 and 173 Torr, consistent with a Doppler fwhm of 430 MHz and an estimated pressure broadening coefficient of  $\sim 0.1 \text{ cm}^{-1} \text{ atm}^{-1}$ .

### Discussion

Cooper<sup>19</sup> has also shown that independent of whether the line profile is Gaussian or Lorentzian, the amplitude of the TTFMS signal is relatively constant for large enough  $\nu_m$ , falling off only when  $\nu_m \lesssim \Gamma_{\text{fwhm}}$ . We therefore would expect that by increasing  $\nu_m$  from 525 MHz to 1.5 GHz the detection limits, expressed in terms of a mixing ratio, should not significantly deteriorate up to pressures of 400–500 Torr, equivalent to atmospheric altitudes of 2–3 km. Expected maximum summer HO<sub>2</sub> mixing ratios under free tropospheric conditions in the tropics range from 20 to 30 pptv.<sup>20</sup> An improvement of 1 order of magnitude in sensitivity would therefore be required before atmospheric open-path measurements (e.g., from mountain tops) would be feasible with the present spectrometer and the present optical path length.

The two strongest lines (14 and 15 in Table I) were found to have absorption cross sections of  $\sim 1.0 \times 10^{-19} \text{ cm}^2 \text{ molecule}^{-1}$ . This corresponds to an integrated line strength of  $S_{\text{line}} = 1.6 \times 10^{-21} \text{ cm}^2 \text{ molecule}^{-1} \text{ cm}^{-1}$  for a Doppler half-width of 215 MHz. This value is at first glance somewhat large for an overtone transition, but earlier work<sup>7</sup> indicates that the strongest lines in the band should occur at these wavelengths. In their Hg-pho-

tosensitized production of HO<sub>2</sub>, Hunziker and Wendt<sup>21</sup> do not quote an absolute HO<sub>2</sub> concentration, but their results are qualitatively consistent with strong unresolved HO<sub>2</sub> absorption bands and thus with the large line strengths reported here.

The line strengths reported here are only smaller by a factor of  $\sim 2$  than those lines measured in the  $\nu_1$  fundamental by Zahniser et al.<sup>5</sup> The lines they observed were within the  $K_a = 1 \leftarrow 0$  and  $K_a = 2 \leftarrow 1$  Q-branch subbands of the  $\perp$ -type  $\nu_1$  fundamental. (As in the present experiment, those measurements were limited by the tuning range of the laser diode.) Since the overtone band is a  $\parallel$ -type transition with strong P and R branches and no Q branch, it is the integrated band strengths that must be compared. It would appear that the overtone band is nearly as intense as the fundamental, though assignment of individual lines and calculation of the overtone band strength is required to confirm this. However, the relatively weak band strength<sup>5</sup> of the fundamental,  $20 \text{ cm}^{-2} (\text{STP atm})^{-1}$ , and the large anharmonicity constant  $\chi_{11}^0 = -112.5 \text{ cm}^{-1}$  both lend credence to this interpretation.<sup>22</sup> Furthermore, a second quantum in the O–H internal coordinate could be expected to produce a considerable change in the dipole moment parallel to the molecular (O–O) axis.

We assume the  $S_{\text{line}} = 1.6 \times 10^{-21} \text{ cm}^2 \text{ molecule}^{-1} \text{ cm}^{-1}$  value will correspond to one of the strongest lines in this band. Accurate wavelength assignment of individual lines is necessary to confirm this. Also, a search for other HO<sub>2</sub> lines in the  ${}^2A'(001) \leftarrow {}^2A''(000)$  vibronic band near  $1.26 \mu\text{m}$ <sup>7</sup> is warranted. Such experiments are presently underway in our laboratory. The importance of HO<sub>2</sub> in atmospheric chemistry merits investigation of all possible methods aimed at monitoring its low concentrations.

*Acknowledgment.* We thank Dr. J. Crowley for helpful discussion regarding the chemistry. This work was supported by the Max Planck Society.

(20) Kanakidou, M.; Singh, H. B.; Valentin, K. M.; Crutzen, P. J. *J. Geophys. Res. D.*, in press.

(21) Hunziker, H. E.; Wendt, H. R. *J. Chem. Phys.* 1976, 64, 3488.  
(22) Levine, I. N. *Molecular Spectroscopy*; John Wiley and Sons: New York, 1975; p 262.

## A Comparative Study of Semiempirical Bond Dissociation Energy Calculations

Harriet F. Ades,<sup>\*,†,‡</sup> Audrey L. Companion,<sup>†</sup> and K. R. Subbaswamy<sup>§</sup>

Center for Computational Sciences and Departments of Chemistry and of Physics and Astronomy,  
University of Kentucky, Lexington, Kentucky 40506-0055 (Received: November 26, 1990)

Anderson's modified version of the extended Hückel molecular orbital method and the MNDO and AM1 methods of Dewar are used to study bond cleavage in molecular fragments of interest in coal liquefaction. Geometric conformations, molecular orbital coefficients for the HOMO's and LUMO's, and bond dissociation energies are computed and compared for the three methods. Qualitative agreement with experiment for bond cleavage is observed for the three methods for the neutral molecule. However the ASED-MO method appears to best describe the bond cleavage in the presence of an electron-accepting catalyst.

### 1. Introduction

A knowledge of relative bond dissociation energies for various bonds in a molecule enables one to predict thermodynamically controlled reaction paths for many reactions. Such bond energies may be obtained from certain quantum chemical methods. Extended Hückel molecular orbital (EHMO) and atom superposition and electron delocalization molecular orbital (ASED-MO) calculations have been successfully used to treat a wide variety of problems, from molecular stability in the gas phase to con-

densed-phase phenomena. The EHMO method has been used to study geometries, isomerism, and rotational barriers for a number of saturated and unsaturated hydrocarbons.<sup>1</sup> The EHMO method with charge iteration was successfully used to predict the most stable absorption site and binding energies of hydrogen in aluminum clusters.<sup>2</sup> Extended Hückel tight binding method calculations have been used to investigate bonding of CH<sub>3</sub>, CH<sub>2</sub>, and CH fragments to Ti, Cr, and Co metal surfaces.<sup>3</sup> Stable adsorption sites were found and migration and coupling reactions

\* Author to whom correspondence should be addressed.

† Center for Computational Sciences.

‡ Department of Chemistry.

§ Department of Physics and Astronomy.

(1) Hoffmann, R. *J. Chem. Phys.* 1963, 39, 1397.

(2) Ades, H. F.; Companion, A. L. *Surf. Sci.* 1986, 177, 553.

(3) Zheng, C.; Apeloig, Y.; Hoffmann, R. *J. Am. Chem. Soc.* 1988, 110, 749.